1521-0111/88/2/347–356$25.00
MOLECULAR PHARMACOLOGY

http://dx.doi.org/10.1124/mol.115.098293
Mol Pharmacol 88:347–356, August 2015



# Role of G Protein–Coupled Receptor Kinases 2 and 3 in μ-Opioid Receptor Desensitization and Internalization

Janet D. Lowe, Helen S. Sanderson, Alexandra E. Cooke, Mehrnoosh Ostovar, Elena Tsisanova, Sarah L. Withey, Charles Chavkin, Stephen M. Husbands, Eamonn Kelly, Graeme Henderson, and Chris P. Bailey

*School of Physiology and Pharmacology, University of Bristol, Bristol, United Kingdom (J.D.L., H.S.S., A.E.C., E.T., S.L.W., E.K., G.H.); Department of Pharmacology, University of Washington School of Medicine, Seattle, Washington (C.C.); and Department of Pharmacy and Pharmacology, University of Bath, Bath, United Kingdom (M.O., S.M.H., C.P.B.)*

Received February 13, 2015; accepted May 26, 2015

## ABSTRACT

There is ongoing debate about the role of G protein–coupled receptor kinases (GRKs) in agonist-induced desensitization of the μ-opioid receptor (MOPr) in brain neurons. In the present paper, we have used a novel membrane-permeable, small-molecule inhibitor of GRK2 and GRK3, Takeda compound 101 (Cmpd101; 3-[[[4-methyl-5-(4-pyridyl)-4*H*-1,2,4-triazole-3-yl] methyl] amino]-*N*-[2-(trifuoromethyl) benzyl] benzamidehydrochloride), to study the involvement of GRK2/3 in acute agonist-induced MOPr desensitization. We observed that Cmpd101 inhibits the desensitization of the G protein–activated inwardly-rectifying potassium current evoked by receptor-saturating concentrations of methionine-enkephalin (Met-Enk), [D-Ala$^2$, N-MePhe$^4$, Gly-ol$^5$]-enkephalin (DAMGO), endomorphin-2, and morphine in rat and mouse locus coeruleus (LC) neurons. In LC neurons from GRK3 knockout mice, Met-Enk–induced desensitization was unaffected, implying a role for GRK2 in MOPr desensitization. Quantitative analysis of the loss of functional MOPrs following acute agonist exposure revealed that Cmpd101 only partially reversed MOPr desensitization. Inhibition of extracellular signal–regulated kinase 1/2, protein kinase C, c-Jun N-terminal kinase, or GRK5 did not inhibit the Cmpd101-insensitive component of desensitization. In HEK 293 cells, Cmpd101 produced almost complete inhibition of DAMGO-induced MOPr phosphorylation at Ser$^{375}$, arrestin translocation, and MOPr internalization. Our data demonstrate a role for GRK2 (and potentially also GRK3) in agonist-induced MOPr desensitization in the LC, but leave open the possibility that another, as yet unidentified, mechanism of desensitization also exists.

## Introduction

The canonical pathway for homologous G protein–coupled receptor (GPCR) desensitization involves agonist activation of the receptor, subsequent G protein activation, G protein–coupled receptor kinase (GRK) translocation to the plasma membrane, phosphorylation of serine and threonine residues primarily on the C-terminal tail of the receptor by GRKs, and arrestin binding to the phosphorylated receptor (Kelly et al., 2008). Although binding of arrestins to the receptor prevents further G protein activation (i.e., desensitizes the receptor–G protein–coupled effector activation pathway), it may also lead to arrestin-mediated signaling and receptor internalization, recycling, and downregulation (Shenoy and Lefkowitz, 2011).

In locus coeruleus (LC) neurons taken from relatively mature animals, [D-Ala$^2$, N-MePhe$^4$, Gly-ol$^5$]-enkephalin (DAMGO), a high-efficacy μ-opioid receptor (MOPr) agonist, induces substantial homologous MOPr desensitization (Llorente et al., 2012). However, despite considerable effort, there remains controversy and confusion around the role of GRKs in the rapid desensitization of neuronal μ-opioid receptors (for extensive review, see Williams et al., 2013). Evidence in favor of a role of GRKs in neuronal MOPr desensitization by agonists with high intrinsic efficacy is 3-fold. First, DAMGO-induced MOPr desensitization in rostral ventromedial medulla neurons

Aspects of this work were supported by grants from the Medical Research Council, UK [Grant MR/J013269/1] and the Biotechnology and Biological Sciences Research Council, UK [Grant BB/J003506/1] to E.K. and G.H.; from the Wellcome Trust, UK (Value in People award) to J.D.L. and C.P.B.; and from the US Public Health Service, National Institutes of Health National Institute on Drug Abuse [Grant R01-DA030074] to C.C.

dx.doi.org/10.1124/mol.115.098293.

This article has supplemental material available at molpharm.aspetjournals.org.

**ABBREVIATIONS:** Cmpd101, Takeda compound 101, 3-[[[4-methyl-5-(4-pyridyl)-4*H*-1,2,4-triazole-3-yl] methyl] amino]-*N*-[2-(trifuoromethyl) benzyl] benzamidehydrochloride; DAMGO, [D-Ala$^2$, N-MePhe$^4$, Gly-ol$^5$]-enkephalin; DNM, dominant-negative mutant; ELISA, enzyme-linked immunosorbent assay; ERK, extracellular signal–regulated kinase; GF109203X, 2-[1-(3-dimethylaminopropyl)indol-3-yl]-3-(indol-3-yl) maleimide; GIRK, G protein–activated inwardly-rectifying potassium; GPCR, G protein–coupled receptor; GRK, G protein–coupled receptor kinase; GSK650394, 2-cyclopentyl-4-(5-phenyl-1*H*-pyrrolo[2,3-*b*]pyridin-3-yl-benzoic acid; HA, hemagglutinin; JNK, c-Jun N-terminal kinase; KO, knockout; LC, locus coeruleus; Met-Enk, methionine-enkephalin; MOPr, μ-opioid receptor; NA, noradrenaline (norepinephrine); PD98059, 2′-amino-3′-methoxyflavone; PDB, pull-down buffer; PKC, protein kinase C; PRK2, protein kinase C–related protein kinase; Ro32-0432, 3-[(8*S*)-8-[(dimethylamino)methyl]-6,7,8,9-tetrahydropyrido[1,2-*a*]indol-10-yl]-4-(1-methyl-1*H*-indol-3-yl)-1*H*-pyrrole-2,5-dione hydrochloride; SGK1, serum and glucocorticoid–regulated kinase; SP600125, anthra[1-9-*cd*]pyrazol-6(2*H*)-one; WGA, wheat germ agglutinin; WT, wild-type; Y-27632, *trans*-4-[(1*R*)-1-aminoethyl]-*N*-4-pyridinylcyclohexanecarboxamide dihydrochloride.

was shown to be inhibited by intracellular perfusion of a GRK2-inhibitory peptide (Li and Wang, 2001). Second, fentanyl-induced MOPr desensitization in the hippocampal dentate gyrus was absent in brain slices from GRK3 knockout (KO) mice (Terman et al., 2004). Third, overexpression of a GRK2 dominant-negative mutant (DNM) in rat LC neurons reduced DAMGO-induced MOPr desensitization (Bailey et al., 2009b). On the other hand, two studies have failed to provide evidence for any involvement of GRKs in MOPr desensitization. Neither heparin, a low-affinity GRK inhibitor, nor staurosporine, a nonselective kinase inhibitor, had any effect on methionine-enkephalin (Met-Enk)–induced MOPr desensitization in rat LC neurons (Arttamangkul et al., 2012). Also, using the GRK2as5 transgenic mouse, in which GRK2 has been mutated to allow chemical inhibition, it was observed that exposure to the inhibitor did not reduce Met-Enk–induced desensitization in LC neurons (Quillinan et al., 2011). However, this transgenic knock-in/chemical inhibition approach would only inhibit GRK2 and not affect GRK3 or other GRKs.

Further complicating the issue, Dang et al. (2009) reported that in rat LC neurons both GRKs and extracellular signal–regulated kinases (ERKs) were involved in MOPr desensitization; inhibition of GRK2/3 by intracellular dialysis of inhibitory peptides or ERK1/2 with a small-molecule ERK1/2 activation inhibitor alone did not reduce Met-Enk–induced desensitization, but with concomitant inhibition of both types of kinase, desensitization was inhibited.

In LC neurons, in vitro morphine, an agonist with lower intrinsic efficacy (McPherson et al., 2010), induced much less MOPr desensitization than high-efficacy opioid agonists (Alvarez et al., 2002; Bailey et al., 2003). The level of morphine-induced desensitization could be enhanced by concomitant activation of protein kinase C (PKC) either indirectly by stimulation of $G_q$-coupled $M_3$ muscarinic receptors or directly with a phorbol ester (Bailey et al., 2004). Expression of the GRK2 DNM did not prevent PKC-mediated MOPr desensitization on morphine application (Bailey et al., 2009b). In contrast, in hippocampal dentate gyrus, GRK3 KO reduced morphine-induced desensitization (Terman et al., 2004).

Until very recently there have been no small-molecule selective, membrane-permeable inhibitors of GRKs. In this paper, we have examined the effects of a novel small-molecule inhibitor of GRK2 and GRK3, Takeda compound 101 (Cmpd101; 3-[[[4-methyl-5-(4-pyridyl)-4*H*-1,2,4-triazole-3-yl] methyl] amino]-*N*-[2-(trifuoromethyl) benzyl] benzamidehydrochloride) (Ikeda et al., 2007; Thal et al., 2011), as well as GRK3 KO and signaling kinase inhibitors, on the rapid desensitization of the MOPr-activated G protein–activated inwardly-rectifying potassium (GIRK) current in LC neurons. We have sought to address several questions relating to the role of GRKs in MOPr desensitization. First, are GRK2 and GRK3 involved in the acute MOPr desensitization induced by high-intrinsic-efficacy agonists, arrestin-biased agonists, and lower-intrinsic-efficacy agonists? Second, do both GRK2 and GRK3 play a role in MOPr desensitization? Third, are multiple kinases such as GRKs and ERKs involved in acute MOPr desensitization?

Our results suggest that GRK2, and potentially GRK3, but not ERK1/2 or c-Jun N-terminal kinase (JNK), are involved in MOPr desensitization by all of the MOPr agonists studied. However, even at concentrations of Cmpd101 that almost completely inhibited MOPr phosphorylation at $Ser^{375}$ and MOPr internalization in HEK 293 cells, the inhibition of agonist-induced loss of functional MOPr in LC neurons was only of the order of 34%.

## Materials and Methods

**Brain Slice Preparation.** Male Wistar rats (5–8 weeks old) were killed by cervical dislocation, and male mice [wild-type (WT) and GRK3 KO mice backcrossed onto C57BL/6 background; 5–8 weeks old] were decapitated under isoflurane-induced anesthesia. Brains were removed and submerged in ice-cold cutting solution containing (in millimolar) 20 NaCl, 2.5 KCl, 0.5 $CaCl_2$, 7 $MgCl_2$, 1.25 $NaH_2PO_4$, 85 sucrose, 25 D-glucose, and 60 $NaHCO_3$; and saturated with 95% $O_2$/5% $CO_2$. Horizontal brain slices (230 $\mu$m thick) containing the LC were prepared using a vibratome (VT1000S; Leica Biosystems, Milton Keynes, UK). Slices were then transferred to artificial cerebrospinal fluid composed of (in millimolar) 126 NaCl, 2.5 KCl, 1.2 $MgCl_2$, 2.4 $CaCl_2$, 1.2 $NaH_2PO_4$, 11.1 D-glucose, 21.4 $NaHCO_3$, and 0.1 ascorbic acid; saturated with 95% $O_2$/5% $CO_2$ at 33°C; and left to equilibrate for at least 1 hour prior to recording. All experiments were performed in accordance with the UK Animals (Scientific Procedures) Act 1986, the European Communities Council Directive 1986 (86/609/EEC), and the University of Bristol and University of Washington ethical review documents as appropriate.

**Whole-Cell Patch-Clamp Recording.** Slices were submerged in a slice chamber (Warner Instruments, Hamden, CT) mounted on a microscope stage (BX51WI; Olympus, Southend-on-Sea, UK) and superfused (2.5–3 ml/min) with artificial cerebrospinal fluid at 33°C. LC neurons were visualized using Nomarski optics using infrared light. Whole-cell patch-clamp recordings were made using electrodes (3–6 MΩ) filled with (in millimolar) 115 K-methylsulfonate, 10 NaCl, 2 $MgCl_2$, 10 HEPES, 6 EGTA, 2 MgATP, and 0.5 $Na_2GTP$ (pH 7.25; osmolarity, 270 mOsm). Recordings of whole-cell currents were filtered at 1 kHz using an Axopatch 200B amplifier (Molecular Devices, Sunnyvale, CA) and analyzed off-line using WinEDR and WinWCP (University of Strathclyde, Glasgow, UK), and pClamp (Molecular Devices).

LC neurons were voltage-clamped at –60 mV with correction for a –12 mV liquid junction potential. Activation of MOPr receptors and $\alpha_2$-adrenoceptors evoked GIRK currents. All drugs were applied in the superfusing solution in known concentrations. In those experiments in which $\alpha_2$ AR responses were studied, noradrenaline (NA) was applied in the presence of prazosin (1 $\mu$M) and cocaine (3 $\mu$M). Because GIRK currents were much smaller in mouse LC, responses in mice were measured in the presence of the glutamate receptor antagonist 6-cyano-7-nitroquinoxaline-2,3-dione (10 $\mu$M) and the $GABA_A$ receptor antagonist bicuculline (10 $\mu$M) to inhibit spontaneous excitatory and inhibitory postsynaptic currents.

**Cell Culture.** Human embryonic kidney 293 cells (HEK 293) cells stably overexpressing hemagglutinin (HA)-tagged rat MOPr (HA-MOPr) were cultured at 37°C in 5% $CO_2$ in Dulbecco's modified Eagle's medium supplemented with 10% fetal bovine serum, 10 U/ml penicillin, 10 mg/ml streptomycin (Invitrogen/Life Technologies, Paisley, UK), and 250 $\mu$g/ml G418 (Geneticin; Merck, Nottingham, UK). Cells were seeded onto 60-mm dishes and grown to 90% confluence, then subjected to serum starvation for 24 hours.

**Wheat Germ Agglutinin Enrichment of HA-MOPr.** Glycosylated HA-MOPr was enriched from cells that were lysed in pull-down buffer (PDB) composed of (in millimolar) 20 HEPES [pH 7.4], 150 NaCl, 1 $Na_3VO_4$, 10 $\beta$-glycerophosphate, 50 NaF, 1 phenylmethanesulfonylfluoride, and 5 EDTA plus 1% Triton X-100, 10% glycerol, 0.1% SDS, 2 $\mu$g/ml leupeptin, 2 $\mu$g/ml aprotinin, and 1 $\mu$g/ml pepstatin A. The protein concentration of clarified cell lysate was adjusted to 1.5 mg/ml and an input sample removed for Western blot analysis. Cell lysate (2.25 mg) was then incubated with 15 $\mu$l sedimented wheat germ agglutinin (WGA)–agarose beads (Sigma-Aldrich, Dorset, UK), prewashed in PDB, and incubated overnight at 4°C. Beads were then washed three times in PDB for 5 minutes at 4°C.

WGA-binding proteins were eluted with the addition of SDS-sample buffer and boiling at 95°C for 4 minutes.

**Western Blotting.** Eluted WGA-binding proteins and input sample were supplemented with β-mercaptoethanol for gel loading. Samples were subjected to SDS-PAGE and proteins transferred onto polyvinylidene fluoride membranes. For detection of agonist-induced receptor phosphorylation, antibodies targeting $pSer^{375}$ on MOPr were used (dilution 1:1000; Cell Signaling Technology, Danvers, MA) and total receptor levels detected with anti-HA antibody (1:1000; Cambridge Bioscience Ltd., Cambridge, UK). For input samples, anti-pERK1/2, anti-ERK1/2, and anti–pElk-1 (each 1:1000; Cell Signaling Technology) and anti-tubulin antibodies were used (1:10,000; Sigma-Aldrich). Following incubation with the species-appropriate horseradish peroxidase–conjugated secondary antibody (donkey anti-rabbit, dilution 1:7500; sheep anti-mouse, 1:10,000; GE Healthcare, Little Chalfont, UK), bands were visualized by enhanced chemiluminescence with SuperSignal West Dura Chemiluminescent Substrate (Thermo Fisher Scientific, Hemel Hempstead, UK). Densitometry of bands was undertaken using ImageJ (NIH, Bathesda, MD); duplicate values were taken for each sample and then averaged. $pSer^{375}$ levels were normalized against corresponding total HA-MOPr levels and pERK1/2 against total ERK1/2 levels determined in the same experiment.

**Internalization Assays.** DAMGO-induced internalization of HA-MOPr was assessed by enzyme-linked immunosorbent assay (ELISA) as previously described (Johnson et al., 2006) and by confocal microscopy imaging (Mundell et al., 2006). HEK 293 cells stably expressing HA-MOPr were prelabeled with primary antibody for 1 hour at 4°C before incubation with Cmpd101 (3 or 30 μM) for 30 minutes at 37°C. Cells were then stimulated with DAMGO (10 μM) at 37°C to induce internalization. In the ELISA, changes in surface receptor expression were subsequently determined by normalizing data from each treatment group to corresponding control surface receptor levels determined from cells not exposed to DAMGO in the same experiment. For confocal imaging, cells were imaged using a Leica SP5-AOBS confocal laser scanning microscope attached to a Leica DM16000 inverted epifluorescence microscope with a pLApoBL 63× oil immersion objective.

**Arrestin Translocation Assay.** For the arrestin-3 recruitment assay, PathHunter cells and accompanying assay kit were obtained from DiscoveRx (Birmingham, UK). These cells are U2OS (human osteosarcoma) cells stably expressing tagged human MOPr and tagged arrestin-3 such that recruitment of arrestin-3 to the receptor leads to reconstitution of β-galactosidase activity, which is measured by luminescence in a plate reader (McPherson et al., 2010). The experiments were undertaken exactly as described in the manufacturer's instructions, with the agonist DAMGO being added to the cells for 90 minutes, and where applicable Cmpd101 being added alone or 30 minutes before DAMGO.

**Kinase Screen.** The express kinase screen was performed at the Medical Research Council International Centre for Kinase Profiling (Dundee, UK). The screen comprised 52 human enzymes providing a representative sampling of the kinome, with the exception of lipid kinases. The method used was a radioactive filter binding assay using $^{32}$ATP, which provides a direct measure of kinase activity (Hastie et al., 2006; Bain et al., 2007). Cmpd101 was studied at a concentration of 1 μM. Results are given as the percentage of kinase activity in the absence of the inhibitor. The ATP concentrations used were at or below the calculated $K_m$ for ATP for each individual kinase. The screen was performed in duplicate, and results are given as a mean value with S.D.

**Quantification of DAMGO-Induced Loss of Functional MOPr.** Following desensitization of MOPr by bath application of DAMGO, DAMGO was replaced by morphine. Using the operational model of agonism (Black et al., 1985), transducer ratio ($\tau$) values for morphine were calculated (as in Bailey et al., 2009a). Percentage loss of receptor responsiveness (f) was then calculated using the equation $f = 100 \times (1 - \tau_2/\tau_1)$, where $\tau_1$ is the value in control slices and $\tau_2$ is the value after DAMGO-induced desensitization (Lohse et al., 1990).

**Statistics.** Data are presented as means ± S.E. and were analyzed by unpaired two-tailed Student's $t$ tests, one-way or two-way analysis of variance with Bonferroni post hoc test as appropriate using Prism 5 (GraphPad Software, Inc., La Jolla, CA). Differences were assumed to be significant at $P < 0.05$.

**Drugs and Compounds.** Cmpd101 hydrochloride was synthesized at the University of Bath (Bath, UK) in nine steps from isonicotinic acid hydrazide (Ikeda et al., 2007). Analysis of the final compound (as the free base) provided data consistent with the structure with purity of >99% (by $^{13}$C NMR): $^1$H NMR (400 MHz, $CDCl_3$) δ 8.71 (dd, $J$ = 1.6 Hz, $J$ = 4.4 Hz, 2H); 7.63–7.45 (m, 5H); 7.34 (t, $J$ = 7.6 Hz, 1H); 7.25–7.24 (m, 1H); 7.18 (t, $J$ = 7.6 Hz, 1H); 7.06 (d, $J$ = 6.8 Hz, 1H); 6.91–6.85 (m, 2H); 4.76 (d, $J$ = 6.00 Hz, 2H); 4.50 (s, 2H); 3.71 (s, 3H); $^{13}$C NMR (100 MHz, $CDCl_3$) δ 167.6, 153.8, 153.2, 150.3, 147.5, 136.6, 135.2, 134.4, 132.3, 130.2, 129.5, 128.1, 127.8, 127.5, 126.0, 125.9, 125.8, 125.7, 123.1, 122.5, 116.6, 116.3, 111.9, 76.7, 40.5, 39.3, 31.6; ESIMS: calculated for $C_{24}H_{21}F_3N_6NaO$, 489.1627; found 489.1701.

Other compounds included DAMGO and Met-Enk (Bachem, Bubendorf, Switzerland); morphine hydrochloride (Macfarlane-Smith, Edinburgh, UK); cocaine hydrochloride (Sigma-Aldrich); endomorphin-2, bicuculline, 6-cyano-7-nitroquinoxaline-2,3-dione disodium, naloxone hydrochloride, noradrenaline bitartrate, prazosin hydrochloride, Y-27632 [*trans*-4-[(1*R*)-1-aminoethyl]-*N*-4-pyridinylcyclohexanecarboxamide dihydrochloride], and amlexanox (Ascent Scientific/Abcam Biochemicals, Cambridge, UK); and GF109203X [2-[1-(3-dimethylaminopropyl)indol-3-yl]-3-(indol-3-yl) maleimide], GSK650394 [2-cyclopentyl-4-(5-phenyl-1*H*-pyrrolo[2,3-*b*]pyridin-3-yl-benzoic acid], and PD98059 [2′-amino-3′-methoxyflavone] (Tocris Bioscience, Bristol, UK). All other reagents were from Sigma-Aldrich.

## Results

**Role of GRK2 and GRK3 in Acute MOPr Desensitization Induced by Met-Enk or DAMGO.** In rat LC neurons, activation of MOPrs by receptor-saturating concentrations of Met-Enk (30 μM), DAMGO (10 μM), or endomorphin-2 (10 μM) elicited outward current through GIRK channels that rapidly desensitized in the presence of the drug, with only ~50% of the initial current remaining after 10 minutes of exposure (Fig. 1). To examine the role of GRK2 and GRK3 in the Met-Enk–induced desensitization, LC slices were pretreated with the inhibitor Cmpd101 at concentrations previously shown to inhibit desensitization of $\beta_2$-adrenoceptors in HEK 293 cells (Ikeda et al., 2007). Cmpd101 concentration-dependently reduced the amount of Met-Enk–induced desensitization (Fig. 1, A–C) such that in the presence of Cmpd101 (30 μM) the desensitization induced by Met-Enk (30 μM) was reduced to only 15%. We also observed that Cmpd101 reduced the amount of desensitization induced by DAMGO (10 μM; Fig. 1, D–F) and endomorphin-2 (10 μM; Fig. 1, G–I).

To determine whether there was any additional role for ERK1/2, PKC, or JNK in MOPr desensitization, we exposed cells to Cmpd101 and PD98059 (10 μM) to inhibit ERK1/2 (Met-Enk as agonist; Fig. 1C), SP600125 [anthra[1-9-*cd*] pyrazol-6(2*H*)-one] (30 μM) to inhibit JNK (Met-Enk as agonist; Fig. 1C), or GF109203X (1 μM) to inhibit PKC (DAMGO as agonist; Fig. 1F). We did not observe any further reduction in desensitization in the presence of the ERK1/2, PKC, or JNK inhibitors. Neither the ERK1/2 nor JNK inhibitor applied on its own in the absence of Cmpd 101 affected Met-Enk–induced desensitization (control: 51 ± 6%, $n$ = 5; + 10 μM PD98059: 43 ± 5%, $n$ = 5; + 30 μM SP600125:

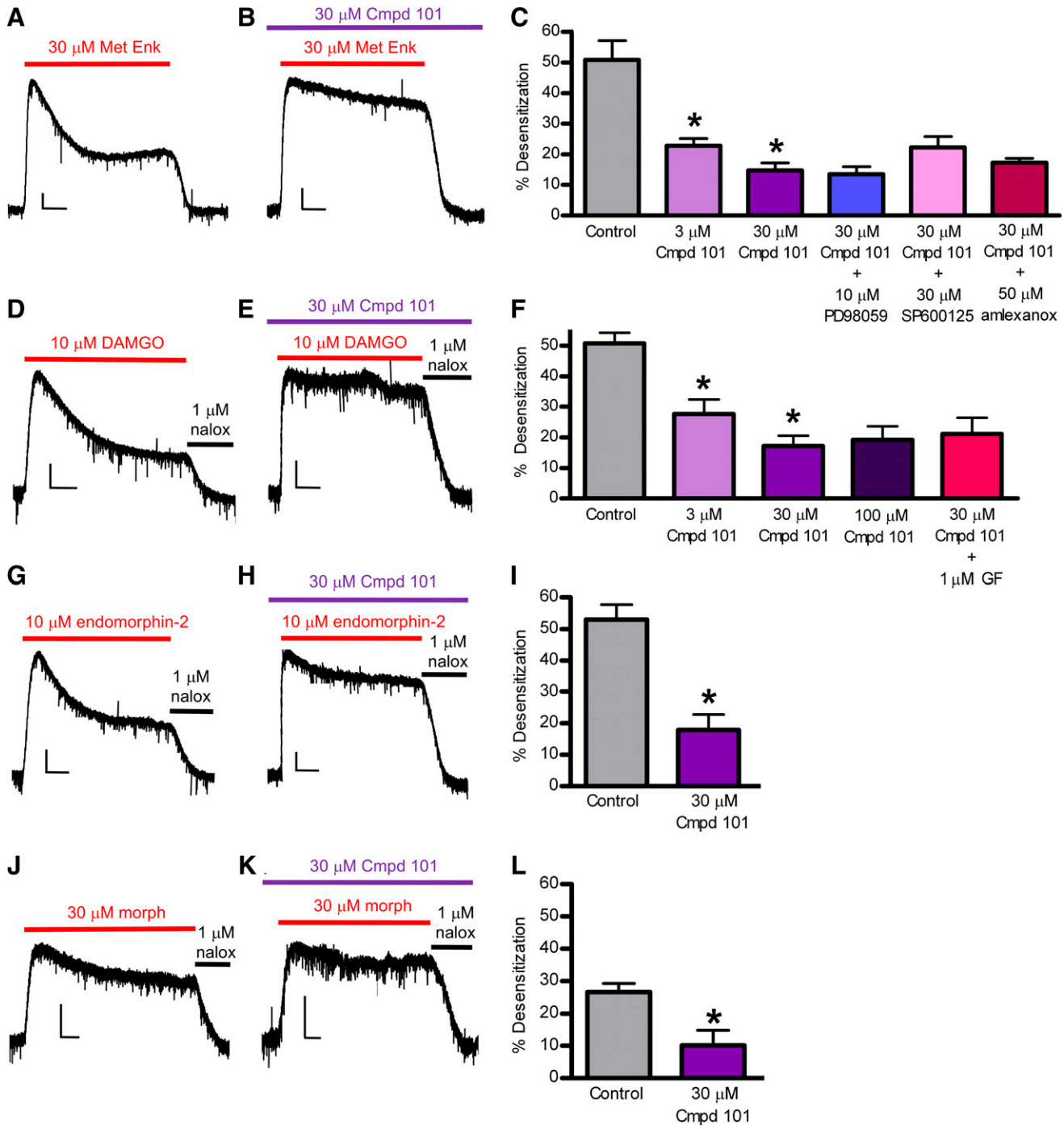


**Fig. 1.** Inhibition of MOPr desensitization by Cmpd101 in rat LC neurons. Traces in (A), (D), (G), and (J) show outward potassium currents recorded from rat LC neurons in response to receptor-saturating concentrations of Met-Enk (30 $\mu$M), DAMGO (10 $\mu$M), endomorphin-2 (10 $\mu$M), and morphine (morph; 30 $\mu$M). The Met-Enk, DAMGO, and endomorphin-2 responses desensitized rapidly over the 10 minutes of agonist application. The desensitization induced by morphine was less than that produced by the other agonists and was measured after 15 minutes of morphine application. Agonist responses returned to baseline after washout (Met-Enk) or when naloxone (nalox; 1 $\mu$M) was applied. The middle column of traces, (B), (E), (H), and (K), show currents induced by each agonist in slices exposed to Cmpd101 (30 $\mu$M) for at least 15 minutes before and during the application of the opioid agonists. Traces in (C), (F), (I), and (L) show pooled data for the percentage desensitization after 10 minutes of Met-Enk, DAMGO, or endomorphin-2 application and 15 minutes of morphine application from experiments such as those illustrated in the two columns of experimental traces. Cmpd101 significantly inhibited the desensitization of all four agonists. Met-Enk: $n = 5$ for all experiments; DAMGO: $n = 4$ for all experiments; endomorphin-2: $n = 6$ for all experiments; morphine: $n = 6$ for all experiments. $^*P < 0.05$, analysis of variance compared with the appropriate control. All scale bars, 50 pA, 2 minutes. GF, GF109203X.

50 ± 4%, $n = 5$). Amlexanox has recently been identified as a GRK5 inhibitor (Homan et al., 2014a). When cells were exposed to Cmpd101 and amlexanox (50 $\mu$M), there was no further reduction in desensitization compared with Cmpd101 alone (Fig. 1C). Amlexanox applied on its own in the absence of Cmpd101 did not affect Met-Enk–induced desensitization

(% Met-Enk–induced desensitization in 50 $\mu$M amlexanox alone: 51 ± 3%, $n$ = 5).

The inhibition of MOPr desensitization that we observed with Cmpd101 does not appear to be due to it acting as a MOPr antagonist to reduce the number of receptors being activated. When a submaximal concentration of Met-Enk (600 nM) was applied before and following exposure of cells to Cmpd101 (3 $\mu$M for 15 minutes), the Met-Enk response in the presence of Cmpd101 was not different from the initial response before Cmpd101 (94 ± 13% of initial response, $n$ = 4, one-sample $t$ test versus 100%, $P > 0.05$).

**Role of GRK2 and GRK3 in Morphine-Induced MOPr Desensitization.** Although morphine produces much less acute MOPr desensitization in LC neurons compared with either Met-Enk or DAMGO (Bailey et al., 2004, 2009b), the morphine response did desensitize by ~25% over a 15-minute application (Fig. 1, J–L). Pretreatment with Cmpd101 (30 $\mu$M) significantly reduced the morphine-induced desensitization. This suggests that GRK2 and GRK3 are not only involved in desensitization to higher-efficacy MOPr agonists such as Met-Enk and DAMGO, but are also involved in desensitization to the partial agonist morphine in the absence of PKC activation.

**MOPr Desensitization in LC Neurons from GRK3 KO Mice.** Cmpd101 was previously shown to be almost equally effective at inhibiting GRK2 and GRK3 (Thal et al., 2011). GRK3 KO has been reported to abolish the desensitization induced by fentanyl and morphine in rat hippocampal dentate gyrus neurons (Terman et al., 2004). To determine whether GRK3 was the sole isoform required for MOPr desensitization in LC neurons, we measured Met-Enk–induced desensitization in LC neurons prepared from GRK3 KO mice. The amplitude of the Met-Enk–induced current was similar in neurons from both GRK3 KO and WT mice (WT: 72 ± 10 pA, $n$ = 6; GRK KO: 58 ± 11 pA, $n$ = 6; $P > 0.05$). Met-Enk–induced desensitization measured after 10 minutes of Met-Enk application was also not significantly different in GRK3 KO neurons compared with WT controls (Fig. 2, A and B). To ensure that there was not a species-specific difference in the mechanism of desensitization, we also examined the ability of Cmpd101 to inhibit Met-Enk–induced desensitization in mouse LC neurons since the previous experiments with Cmpd101 were performed in rat LC neurons. In LC neurons from C57BL/6J WT mice, Met-Enk produced a similar amount of desensitization (45%) to that observed in rat neurons after a 10-minute application. Cmpd101 inhibited the Met-Enk–induced desensitization in WT mouse LC neurons, being maximally effective at the lower (3 $\mu$M) concentration (Fig. 2, C and D).

These results suggest first that GRK2 plays a role in Met-Enk–induced desensitization in LC neurons and second either that GRK3 plays no role in Met-Enk–induced desensitization in LC neurons or that GRK3 is not solely responsible. However, as Cmpd101 is a mixed GRK2/3 inhibitor, we cannot exclude the possibility that both GRK2 and GRK3 are involved and that removal of only one (in our current experiments GRK3) is insufficient to inhibit desensitization.

**Loss of Functional MOPrs Underlying Acute MOPr Desensitization.** There is a significant MOPr reserve in LC neurons that needs to be removed (i.e., desensitized) before any decrease in the response to a supramaximal concentration of a full agonist such as Met-Enk or DAMGO can be detected, and therefore the true proportion of receptors that have been desensitized is hard to assess from responses such as those shown in Fig. 1 (Connor et al., 2004). To determine the actual loss of functional MOPrs following desensitization, we used a previously developed protocol that measures the decrease induced by desensitization of the maximum response to the partial agonist morphine (Bailey et al., 2009a). For a partial agonist, the maximum response occurs when all the receptors are occupied, and therefore any decrease in maximum response is directly related to a loss of receptor function. To be able to compare results from different neurons,

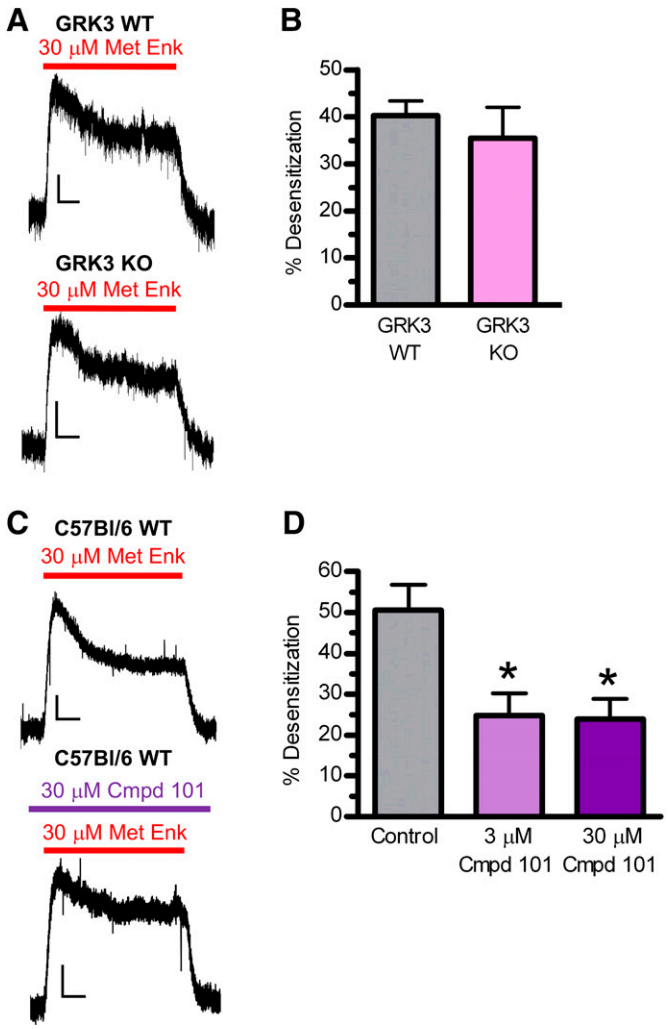


**Fig. 2.** Effect of GRK3 KO and Cmpd101 on Met-Enk–induced MOPr desensitization in mouse LC neurons. (A) Representative potassium currents in response to a receptor-saturating concentration of Met-Enk (30 $\mu$M) recorded from mouse LC neurons in slices taken from either WT (top) or GRK3 KO (bottom) mouse brains. (B) Pooled data from experiments as illustrated in (A). The desensitization induced by Met-Enk over a 10-minute application was not different in GRK3 KO mice compared with WT littermate controls (GRK3 WT, $n$ = 6; GRK3 KO, $n$ = 6; $t$ test, $P > 0.05$). (C) Representative potassium currents in response to Met-Enk (30 $\mu$M) recorded from LC neurons from slices taken from C57BL/6J mice that were either untreated (top) or pretreated with Cmpd101 (30 $\mu$M) for at least 15 minutes prior to and during the application of Met-Enk (bottom). (D) Pooled data for the percentage desensitization over the 10 minutes of opioid agonist application from experiments such as those illustrated in (C). Cmpd101 (3 and 30 $\mu$M) significantly inhibited Met-Enk–induced desensitization measured after 10 minutes of agonist application. $n$ = 5 for each; *$P < 0.05$, analysis of variance compared with control. All scale bars, 15 pA, 2 minutes.

the morphine response in each was normalized to the response to NA (100 $\mu$M), which activates $\alpha_2$-adrenoceptors that couple to the same pool of GIRKs in LC neurons (North and Williams, 1985).

In control LC neurons, the maximum response evoked by morphine was 85% of the maximum response to NA (100 $\mu$M) (Fig. 3A). To examine the reduction in morphine response caused by DAMGO-induced MOPr desensitization, neurons were first treated with DAMGO (10 $\mu$M) for 12 minutes to induce desensitization, then the maximum response to morphine (30 $\mu$M) was determined at plateau (6 minutes after DAMGO was replaced by morphine; Fig. 3, B and C). In neurons that were first treated with DAMGO (10 $\mu$M) for 12 minutes to induce desensitization, the maximum response to morphine was reduced by >80% (Fig. 3B). Using the operational model of agonism (Black et al., 1985) to estimate the actual loss of functional MOPrs induced by DAMGO (for details, see Bailey et al., 2009a and *Materials and Methods*), we calculate that the DAMGO treatment induced a 93% loss of functional MOPrs. When we repeated the experiment but this time in the presence of Cmpd101 (3 or 30 $\mu$M), the desensitization induced by DAMGO was markedly reduced, as was the reduction in the maximum response to morphine (Fig. 3, C and D). In the presence of 30 $\mu$M Cmpd101, the desensitization induced by DAMGO (10 $\mu$M) reduced the maximum response to morphine by only 44%, which equates to a 59% loss of functional MOPrs. Thus, while Cmpd101 reduced the DAMGO-induced loss of functional receptors from 93 to 59%, this reduction was sufficient to produce a marked reduction in the desensitization observed during application of a receptor-saturating concentration of agonist (Fig. 1).

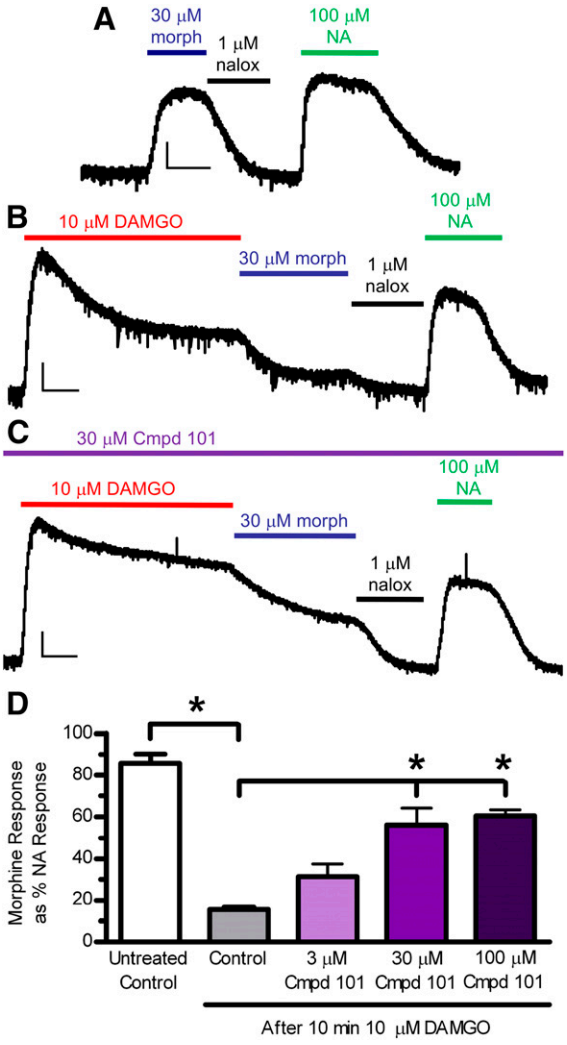


**Fig. 3.** Cmpd101 reduced the depression of the maximum response to morphine produced by DAMGO-induced desensitization. (A and B) Representative potassium current traces showing the amplitude of the maximum response to morphine (morph) compared with that of NA (100 $\mu$M) in the absence of (A) or after induction of desensitization induced by application of (B) DAMGO (10 $\mu$M for 12 minutes). The opioid antagonist naloxone (nalox, 1 $\mu$M) was added after morphine to bring the response back to baseline prior to application of NA. (C) Representative current trace from an experiment in which slices were exposed to Cmpd101 (30 $\mu$M) for at least 15 minutes before and during the application of the opioid agonists. (D) Pooled data from experiments as illustrated in (A–C). DAMGO-induced desensitization inhibited the maximum response to morphine. Cmpd101 concentration-dependently reversed the DAMGO desensitization–induced decrease in the morphine response. $n$ = 4 for all experiments; *$P < 0.05$, analysis of variance. All scale bars, 60 pA, 2 minutes.

Overall, our findings with Cmpd101 suggest that GRK2 and possibly also GRK3 are involved in both Met-Enk– and DAMGO-induced desensitization of MOPr, but it is clear that there is a component of desensitization that remains in the presence of the drug either because of incomplete inhibition of GRK2 and GRK3 by Cmpd101 or because an additional Cmpd101-resistant mechanism of desensitization exists.

**MOPr Phosphorylation, Internalization, and Arrestin Translocation.** To assess the ability of Cmpd101 to inhibit GRK in intact cells, we next examined agonist-induced MOPr phosphorylation, arrestin translocation, and MOPr internalization. Because these processes are more difficult to assess in neurons in a brain slice, we instead examined them in cell lines stably expressing MOPrs. Phosphorylation of HA-tagged MOPr was measured by Western blotting using the commercially available antibody that recognizes the phosphorylated residue $Ser^{375}$ in the MOPr C-terminal tail. We have previously demonstrated that in vitro GRK2 directly phosphorylates $Ser^{375}$ (Chen et al., 2013). Application of DAMGO (10 $\mu$M) for 5 minutes produced a robust phosphorylation of $Ser^{375}$ that was partially inhibited by pretreatment of cells for 30 minutes with 3 $\mu$M Cmpd101 and fully blocked by pretreatment with 30 $\mu$M Cmpd101 (Fig. 4, A and B). Cmpd101 (30 $\mu$M) also prevented phosphorylation of MOPr at $Thr^{370}$, $Thr^{376}$, and $Thr^{379}$ residues also known to be phosphorylated by GRKs (H. S. Sanderson and E. Kelly, unpublished observations).

Translocation of arrestin-3 to agonist-activated MOPr was assessed using the DiscoveRx PathHunter assay. Application of DAMGO (10 $\mu$M for 90 minutes) led to a large recruitment of arrestin-3 to MOPr, which was dramatically reduced by in the presence of Cmpd101 (30 $\mu$M) (Fig. 4C).

We assessed internalization of HA-tagged MOPrs by ELISA and confocal microscopy using an anti-HA antibody to label surface receptors. DAMGO (10 $\mu$M) application induced MOPr internalization in a time-dependent manner, and Cmpd101 markedly reduced DAMGO-induced MOPr internalization (Fig. 4, D and E).

These data demonstrate that Cmpd101 was able to block DAMGO-induced MOPr phosphorylation on $Ser^{375}$, arrestin recruitment, and MOPr internalization presumably by inhibiting GRK2 and GRK3. This contrasts somewhat with our

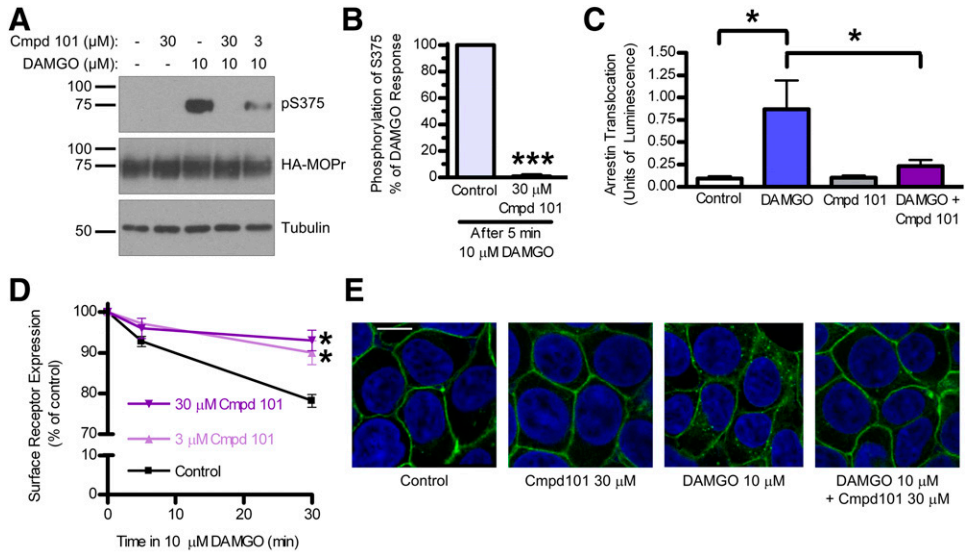


**Fig. 4.** Inhibition of DAMGO-induced MOPr phosphorylation and arrestin recruitment by Cmpd101. (A) HEK 293 cells stably expressing HA-tagged rat MOPr were pretreated with Cmpd101 for 30 minutes prior to stimulation with DAMGO (10 $\mu$M for 5 minutes). Agonist-induced phosphorylation was assessed by Western blot analysis using an antibody targeting phospho-Ser$^{375}$ (pS375). Anti-HA and anti-tubulin antibodies confirmed equal loading of the gels. (B) Western blots as illustrated in (A) were quantified by densitometry and expressed as a percentage of the maximal phosphorylation in response to DAMGO (10 $\mu$M) in each experiment. Cmpd101 (30 $\mu$M) abolished DAMGO-induced MOPr phosphorylation at Ser$^{375}$ ($n = 3$; ***$P < 0.001$, analysis of variance (ANOVA) compared with control + DAMGO). No phosphorylation was seen under control conditions or with Cmpd101 alone ($n = 3$). (C) DAMGO-induced arrestin-3 translocation to the receptor was measured using the DiscoveRx PathHunter assay. DAMGO (10 $\mu$M) application produced a robust recruitment of arrestin-3 to the receptor that was significantly inhibited in cells that were pretreated with Cmpd101 (30 $\mu$M) for 30 minutes ($n = 3$; *$P < 0.05$, ANOVA). (D) Internalization of HA-MOPrs expressed in HEK 293 cells assessed by ELISA using an anti-HA antibody to label surface receptors. DAMGO (10 $\mu$M) induced a time-dependent loss of surface receptors that was significantly inhibited by Cmpd101 ($n = 3$–4; *$P < 0.05$, ANOVA compared with control). (E) Confocal images of HA-MOPrs following incubation with anti-HA antibody and fluorescein-tagged secondary antibody (green), counterstained with Hoechst 33258 nucleic acid stain (blue) following incubation with DAMGO (10 $\mu$M) and/or Cmpd101 (30 $\mu$M). Images are from one experiment repeated 3 times. Scale bar, 10 $\mu$M.

data from LC neurons, in which although Cmpd101 could reduce agonist-induced desensitization, the extent of the reduction was only ~34% when calculated as loss of functional receptors.

**ERK1/2 Phosphorylation.** It has previously been reported that GRK2 and GRK3 inhibition alone was not sufficient to inhibit Met-Enk–induced desensitization in mouse LC neurons but that a combination of GRK2, GRK3, and ERK1/2 inhibition was required; i.e., there was overlap and redundancy between GRK and ERK1/2 in MOPr desensitization (Dang et al., 2009). To confirm that Cmpd101 did not inhibit ERK1/2 activity, we measured both the phosphorylation of ERK1/2, which is often used as a measure of its activity (Roskoski, 2012), and the phosphorylation of Elk-1 by ERK1/2 (Cruzalegui et al., 1999) in HEK 293 cells stably expressing HA-tagged MOPrs. Cmpd101 did not affect the DAMGO-induced (10 $\mu$M, 5 minutes) increase in ERK1/2 phosphorylation (Fig. 5, A and B). Moreover, at 30 $\mu$M, Cmpd101 on its own produced a small increase in basal ERK1/2 phosphorylation (Fig. 5, A and B). Similarly, Cmpd101 (30 $\mu$M) did not inhibit the DAMGO-induced (10 $\mu$M, 5 minutes) increase in Elk-1 phosphorylation (Fig. 5, C and D). The ERK1/2 activation inhibitor PD98059 significantly decreased both DAMGO-induced ERK1/2 and Elk-1 phosphorylation (Fig. 5E).

Thus, the ability of Cmpd101 to decrease MOPr desensitization in the LC is unlikely to be due to an inhibition of ERK1/2 activity in combination with the inhibition of GRK activity.

**Selectivity of Kinase Inhibition by Cmpd101.** Cmpd101 has previously been shown to be highly selective for GRK2 and GRK3 over other GRK isoforms (Ikeda et al., 2007; Thal et al., 2011). We subjected Cmpd101 to a further kinase screen at the Medical Research Council International Centre for Kinase Profiling (Dundee, UK) to determine whether it inhibited the activity of other non-GRK kinases. As this screen was conducted on purified kinases in vitro, we performed the screen using 1 $\mu$M Cmpd101 (i.e., 30× the reported $IC_{50}$ for inhibition of GRK2 in in vitro purified enzyme assay conditions). Of the kinases that have previously been implicated in MOPr desensitization, Cmpd101 inhibited the activity of PKC, protein kinase A, JNK, calcium/calmodulin-dependent protein kinase, and ERK1/2 in vitro by <20% at 1 $\mu$M (Supplemental Fig. 1; Supplemental Table 1). Cmpd101 inhibited only five off-target kinases by >50%; these included protein kinase C–related protein kinase (PRK2) and serum and glucocorticoid-regulated kinase (SGK1), which were inhibited by 93 and 69%, respectively. To test whether either of these kinases might be involved in DAMGO-induced desensitization, we pretreated rat LC slices with established inhibitors of these kinases. GSK650394 (10 $\mu$M) is an inhibitor of SGK1, and Y-27632 (50 $\mu$M) is an inhibitor of both PRK2 and Rho-associated protein kinase 2, which Cmpd101 also inhibited by 47% in the kinase screen. LC neurons pretreated with a combination of these two kinase inhibitors did not show any difference in the amount of desensitization induced by a 10-minute application of DAMGO (30 $\mu$M) compared with that observed in control neurons (Supplemental Fig. 2). Therefore, these off-target actions of Cmpd101 do not appear to play a role in the inhibition of MOPr desensitization by Cmpd101.

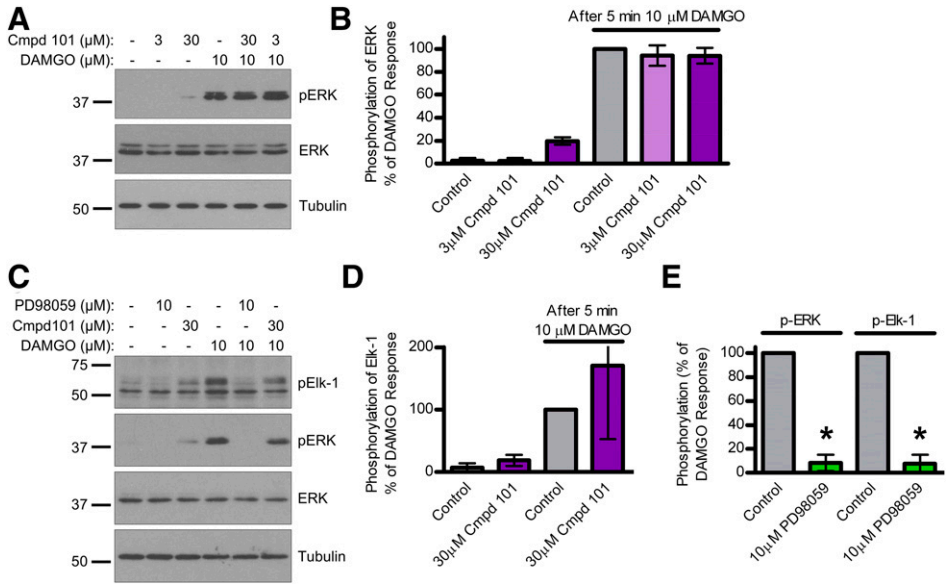


**Fig. 5.** Effect of Cmpd101 on the phosphorylation of ERK1/2 and Elk-1. (A) ERK1/2 activity in HEK 293 cells expressing HA-MOPrs was assessed by Western blot using an antibody targeting phospho-ERK1/2. DAMGO (10 $\mu$M) application for 5 minutes produced a robust phosphorylation of ERK1/2 in both control cells and cells that had been pretreated with Cmpd101 for 30 minutes. Antibodies against total ERK1/2 and tubulin confirmed equal loading of the gels. (B) Western blots as illustrated in (A) were quantified by densitometry and expressed as a percentage of the maximal ERK1/2 phosphorylation in response to DAMGO (10 $\mu$M) in each experiment. Cmpd101 did not affect DAMGO-induced ERK1/2 phosphorylation ($P > 0.05$, analysis of variance), but at the higher 30 $\mu$M concentration, Cmpd101 produced a modest but significant activation of ERK1/2 on its own ($P < 0.05$, one-sample $t$ test versus control; $n = 4$ for each). (C) Phosphorylation of the ERK1/2 substrate Elk-1 in response to DAMGO was assessed by Western blot using an antibody targeting pSer$^{383}$ (of Elk-1). Treatment of HA-MOPr cells with DAMGO (10 $\mu$M) for 5 minutes produced phosphorylation of Elk-1, which was unaffected by pretreatment with Cmpd101 (30 $\mu$M) for 30 minutes. In contrast, agonist-dependent phosphorylation of both Elk-1 and ERK1/2 was significantly reduced following pretreatment of 30 minutes with the MEK1 inhibitor PD98059 (10 $\mu$M). Antibodies against total ERK1/2 and tubulin confirmed equal loading of the gels. (D) Western blots of pElk-1 as shown in (C) were quantified by densitometry and expressed as a percentage of the maximal Elk-1 phosphorylation in response to DAMGO (10 $\mu$M) in each experiment. Cmpd101 did not reduce DAMGO-induced Elk-1 phosphorylation at a concentration of 30 $\mu$M ($n = 3$). (E) The ERK1/2 inhibitor PD98059 (10 $\mu$M) reduced both DAMGO-induced pElk-1 and pERK1/2 activation to basal levels. Data as in (C) were quantified by densitometry. *$P < 0.05$, one-sample $t$ test versus control; $n = 3$.

## Discussion

We have studied the effects of Cmpd101, a novel membrane-permeable, small-molecule inhibitor of both GRK2 and GRK3, on agonist-induced MOPr desensitization in LC neurons. Cmpd101 has previously been reported to be a potent inhibitor of GRK2 and GRK3, with reported $IC_{50}$ values of 35 nM (Ikeda et al., 2007) or 290 nM (Thal et al., 2011) under different in vitro purified enzyme assay conditions, but has no activity against GRK5 at concentrations up to 125 $\mu$M (Thal et al., 2011). In intact cell assay conditions, higher concentrations are required, with Cmpd101 showing concentration-dependent inhibition of $\beta_2$-adrenoceptor desensitization in HEK 293 cells over the range 3–30 $\mu$M (Ikeda et al., 2007).

In our preliminary kinase screen, Cmpd101 showed high selectivity when tested across a broad range of kinases, with only the AGC kinases PRK2, mitogen- and stress-activated protein kinase 1, and SGK1 being inhibited by >50% in the presence of 1 $\mu$M Cmpd101. These kinases all sit in regions of the kinome (Manning et al., 2002) close to GRK2 and GRK3 (see Supplemental Fig. 1), although PRK2 and SGK1 appear to play no role in MOPr desensitization (see Supplemental Fig. 2). Other approaches previously taken to inhibit GRKs include the broad-spectrum kinase inhibitor staurosporine (Arttamangkul et al., 2012), the PKC/GRK inhibitor Ro32-0432 [3-[(8*S*)-8-[(dimethylamino)methyl]-6,7,8,9-tetrahydropyrido[1,2-*a*]indol-10-yl]-4-(1-methyl-1*H*-indol-3-yl)-1*H*-pyrrole-2,5-dione hydrochloride] (Hull et al., 2010), "$\beta$-ARK-1 inhibitor" (Iino et al., 2002; Hull et al., 2010), and the antidepressant drug paroxetine (Thal et al., 2012; Homan et al., 2014b). However, none of these approaches combine the cell-permeability, potency, and selectivity profiles of Cmpd101. Moreover, Cmpd101 shows specificity between GRK2/3 and GRK5. Across a range of opioid agonists with different intrinsic efficacies for G protein activation (Met-Enk, DAMGO, and morphine) and arrestin bias (endomorphin-2), we observed that Cmpd101 reduced the desensitization of the opioid-activated GIRK current, indicating the involvement of GRK2 and/or GRK3 in this desensitization. The effective concentrations of Cmpd101 in these whole-cell assays were 100- to 1000-fold higher than the concentrations that inhibit GRK2 and GRK3 in vitro. This likely results from low permeability of the molecule across the cell membrane but could also be due to other factors, such as differences in the conformation or properties of the kinases in a cellular environment.

Our observation that MOPr desensitization in LC neurons was unaffected by GRK3 KO indicates that in these neurons GRK3 is not solely responsible for MOPr desensitization. This observation is different from what has been reported previously in the hippocampal dentate gyrus, where fentanyl-induced MOPr desensitization was absent in brain slices prepared from GRK3 KO mice (Terman et al., 2004), suggesting that different mechanisms of MOPr desensitization may be present in different brain regions. This difference could result from differential expression of GRK isoforms in different neuronal populations. In situ hybridization studies in rats have shown ubiquitous expression of GRK2, -3, and -6 throughout the brain (Erdtmann-Vourliotis et al., 2001), with

expression of GRK2, -3, -5, and -6 in the LC, but no studies have performed quantitative analysis of GRK isoform protein levels in different brain regions. Although GRK2 KO is embryonic-lethal, selective inhibition of GRK2 in the GRK2as5 transgenic mouse has also been reported not to affect Met-Enk–induced desensitization in LC neurons (Quillinan et al., 2011). Further, although overexpression of a GRK2 DNM reduced DAMGO-induced MOPr desensitization in rat LC neurons (Bailey et al., 2009b), this DNM construct is likely to also inhibit GRK3, based on homology of the GRK2 and GRK3 isoforms. Given that Cmpd101 is a potent inhibitor of both GRK2 and GRK3, our data suggest that in LC neurons there is an overlap and redundancy of GRK2 and GRK3 such that KO of only one (e.g., GRK3) is insufficient to inhibit desensitization.

Cmpd101 inhibited agonist-induced phosphorylation of MOPr at $Ser^{375}$ and the subsequent internalization of the receptor in HEK 293 cells. Several groups have previously demonstrated that GRK2 and GRK3 rapidly phosphorylate MOPr. Purified GRK2 phosphorylates $Ser^{375}$ in the C-terminal tail in vitro (Chen et al., 2013). Using phosphosite-specific antibodies, DAMGO and other higher-efficacy agonists have been observed to phosphorylate several amino acid residues in the C-terminal tail of MOPr (Doll et al., 2011, 2012; Just et al., 2013). Phosphorylation at $Ser^{375}$ appears to be the initiating event, but thereafter flanking residues ($Thr^{370}$, $Thr^{376}$, and $Thr^{379}$) are subsequently phosphorylated in a hierarchical manner. This higher-order phosphorylation has been shown to be mediated by GRK2 and GRK3 in that it is reduced by small interfering RNA knockdown of these GRK isoforms. Furthermore, mutation of $Ser^{375}$, $Thr^{376}$, and $Thr^{379}$ to Ala prevented DAMGO-induced MOPr internalization in medium spiny striatal neurons (Just et al., 2013). Morphine, a MOPr partial agonist in the LC, has previously been shown to produce much less acute MOPr desensitization in LC neurons (Alvarez et al., 2002; Bailey et al., 2003) than high-efficacy MOPr agonists. It has also been shown to induce less phosphorylation of $Ser^{375}$, no phosphorylation of $Thr^{376}$ or $Thr^{379}$ (Just et al., 2013), and less arrestin translocation (McPherson et al., 2010). In the present study, we observed that Cmpd101 partially inhibited morphine-induced MOPr desensitization in LC neurons.

Our studies with Cmpd101 support the view that GRK2 and GRK3 do play a role in MOPr desensitization in LC neurons. What was surprising is that when we calculated the loss of MOPr function resulting from agonist-induced desensitization, we found that Cmpd101 only partially reversed the loss of MOPr function that underlies the desensitization. The inability of Cmpd101 to fully reverse the loss of MOPr function induced by DAMGO could indicate either that there are two mechanisms of MOPr desensitization—one involving GRK-mediated phosphorylation (inhibited by Cmpd101) and one that does not involve GRK2 and GRK3—or that, in intact neurons, for reasons that are unclear, Cmpd101 does not completely inhibit GRK2 and GRK3. Evidence against the incomplete GRK inhibition hypothesis would be that in HEK 293 cells Cmpd101 very effectively reduced DAMGO-induced MOPr phosphorylation, arrestin translocation, and MOPr internalization. However, one caveat to this is that, by necessity, the phosphorylation, translocation, and internalization studies were performed under very different experimental conditions to the electrophysiological experiments. If there is a second mechanism involved in MOPr desensitization, this is currently unidentified, but it does not involve ERK1/2, PKC, or JNK, as in the present study inhibitors of these kinases did not reduce MOPr desensitization further in the presence of Cmpd101. One potential alternative mechanism for the residual component of MOPr desensitization is that catalytically inactive GRK2/3 binds $\beta\gamma$ subunits of the G protein, inhibiting GIRK channel function (Raveh et al., 2010); while we cannot rule this out, previous work suggests that this process does not play a role in rat LC neurons of this age (Llorente et al., 2012). Of the other GRK subtypes expressed in mammalian neurons (GRK5 and GRK6), our data suggest that GRK5 is not responsible, as the GRK5 inhibitor amlexanox was ineffective. Although amlexanox lacks specificity (Reilly et al., 2013), and we have no direct proof that it is permeating LC neurons in the slice, it has been shown to inhibit intracellular GRK5-mediated responses, with near complete block at 50 $\mu$M (Homan et al., 2014a). It is not currently known if amlexanox also inhibits the structurally similar GRK6, although previous studies (Bailey et al., 2009a) have shown no effect of GRK6 on MOPr desensitization using viral transfection of the GRK6 DNM.

We have been unable to obtain any evidence to support the view that ERK1/2 participate in MOPr desensitization, as proposed by Dang et al. (2009). In our preliminary in vitro kinase screen, Cmpd101 did show some inhibition of both ERK1 and ERK2, but this was modest (20% inhibition), with a concentration of Cmpd101 that would inhibit GRK2 by >90%. However, we found no evidence in intact cells that Cmpd101 could decrease ERK1/2 phosphorylation or inhibit the phosphorylation of Elk-1 by ERK1/2. Thus, we have excluded the possibility that Cmpd101 inhibits MOPr desensitization by inhibiting both GRK2/3 and ERK1/2.

In conclusion, we demonstrate that Cmpd101 offers a simple means to study the roles of GRK2/3 in GPCR desensitization and other cellular functions. We show here that a component of MOPr desensitization in rodent LC neurons is GRK2/3-mediated. Data from GRK3 KO mice demonstrate that GRK3 ablation alone is insufficient to inhibit MOPr desensitization in these neurons, suggesting either a selective role for GRK2 or redundancy of action between GRK2 and GRK3. The development of a membrane-permeable, small-molecule inhibitor of GRK2/3 gives the opportunity to explore the roles of these kinases in desensitization of MOPRs, and other GPCRs, in native tissues and in vivo.

#### Acknowledgments

The authors thank John Tesmer (University of Michigan, Ann Arbor, MI) for help and guidance with the synthesis of compound 101.

#### Authorship Contributions

*Participated in research design:* Bailey, Kelly, Lowe, Henderson.

*Conducted experiments:* Cooke, Kelly, Lowe, Sanderson, Withey, Tsisanova.

*Contributed new reagents or analytic tools:* Chavkin, Husbands, Ostovar.

*Performed data analysis:* Cooke, Kelly, Lowe, Sanderson, Tsisanova.

*Wrote or contributed to the writing of the manuscript:* Lowe, Kelly, Henderson, Bailey.

#### References

Alvarez VA, Arttamangkul S, Dang V, Salem A, Whistler JL, Von Zastrow M, Grandy DK, and Williams JT (2002) mu-Opioid receptors: ligand-dependent activation of

potassium conductance, desensitization, and internalization. *J Neurosci* **22**: 5769–5776.
Arttamangkul S, Lau EK, Lu HW, and Williams JT (2012) Desensitization and trafficking of $\mu$-opioid receptors in locus ceruleus neurons: modulation by kinases. *Mol Pharmacol* **81**:348–355.
Bailey CP, Couch D, Johnson E, Griffiths K, Kelly E, and Henderson G (2003) Mu-opioid receptor desensitization in mature rat neurons: lack of interaction between DAMGO and morphine. *J Neurosci* **23**:10515–10520.
Bailey CP, Kelly E, and Henderson G (2004) Protein kinase C activation enhances morphine-induced rapid desensitization of mu-opioid receptors in mature rat locus ceruleus neurons. *Mol Pharmacol* **66**:1592–1598.
Bailey CP, Llorente J, Gabra BH, Smith FL, Dewey WL, Kelly E, and Henderson G (2009a) Role of protein kinase C and mu-opioid receptor (MOPr) desensitization in tolerance to morphine in rat locus coeruleus neurons. *Eur J Neurosci* **29**:307–318.
Bailey CP, Oldfield S, Llorente J, Caunt CJ, Teschemacher AG, Roberts L, McArdle CA, Smith FL, Dewey WL, and Kelly E et al. (2009b) Involvement of PKC alpha and G-protein-coupled receptor kinase 2 in agonist-selective desensitization of mu-opioid receptors in mature brain neurons. *Br J Pharmacol* **158**:157–164.
Bain J, Plater L, Elliott M, Shpiro N, Hastie CJ, McLauchlan H, Klevernic I, Arthur JS, Alessi DR, and Cohen P (2007) The selectivity of protein kinase inhibitors: a further update. *Biochem J* **408**:297–315.
Black JW, Leff P, Shankley NP, and Wood J (1985) An operational model of pharmacological agonism: the effect of E/[A] curve shape on agonist dissociation constant estimation. *Br J Pharmacol* **84**:561–571.
Chen YJ, Oldfield S, Butcher AJ, Tobin AB, Saxena K, Gurevich VV, Benovic JL, Henderson G, and Kelly E (2013) Identification of phosphorylation sites in the COOH-terminal tail of the $\mu$-opioid receptor. *J Neurochem* **124**:189–199.
Connor M, Osborne PB, and Christie MJ (2004) Mu-opioid receptor desensitization: is morphine different? *Br J Pharmacol* **143**:685–696.
Cruzalegui FH, Cano E, and Treisman R (1999) ERK activation induces phosphorylation of Elk-1 at multiple S/T-P motifs to high stoichiometry. *Oncogene* **18**: 7948–7957.
Dang VC, Napier IA, and Christie MJ (2009) Two distinct mechanisms mediate acute mu-opioid receptor desensitization in native neurons. *J Neurosci* **29**:3322–3327.
Doll C, Konietzko J, Pöll F, Koch T, Höllt V, and Schulz S (2011) Agonist-selective patterns of $\mu$-opioid receptor phosphorylation revealed by phosphosite-specific antibodies. *Br J Pharmacol* **164**:298–307.
Doll C, Pöll F, Peuker K, Loktev A, Glück L, and Schulz S (2012) Deciphering $\mu$-opioid receptor phosphorylation and dephosphorylation in HEK293 cells. *Br J Pharmacol* **167**:1259–1270.
Erdtmann-Vourliotis M, Mayer P, Ammon S, Riechert U, and Höllt V (2001) Distribution of G-protein-coupled receptor kinase (GRK) isoforms 2, 3, 5 and 6 mRNA in the rat brain. *Brain Res Mol Brain Res* **95**:129–137.
Hastie CJ, McLauchlan HJ, and Cohen P (2006) Assay of protein kinases using radiolabeled ATP: a protocol. *Nat Protoc* **1**:968–971.
Homan KT, Wu E, Cannavo A, Koch WJ, and Tesmer JJ (2014a) Identification and characterization of amlexanox as a G protein-coupled receptor kinase 5 inhibitor. *Molecules* **19**:16937–16949.
Homan KT, Wu E, Wilson MW, Singh P, Larsen SD, and Tesmer JJ (2014b) Structural and functional analysis of G protein-coupled receptor kinase inhibition by paroxetine and a rationally designed analog. *Mol Pharmacol* **85**:237–248.
Hull LC, Llorente J, Gabra BH, Smith FL, Kelly E, Bailey C, Henderson G, and Dewey WL (2010) The effect of protein kinase C and G protein-coupled receptor kinase inhibition on tolerance induced by mu-opioid agonists of different efficacy. *J Pharmacol Exp Ther* **332**:1127–1135.
Iino M, Furugori T, Mori T, Moriyama S, Fukuzawa A, and Shibano T (2002) Rational design and evaluation of new lead compound structures for selective betaARK1 inhibitors. *J Med Chem* **45**:2150–2159.
Ikeda S, Keneko M, and Fujiwara S (2007) inventors, Takeda Pharmaceutical Co. Ltd., Ikeda S, Keneko M, Fujiwara S, assignees. Cardiotonic agent comprising GRK inhibitor. International patent WO 2007034846. 2007 Mar 29.
Johnson EA, Oldfield S, Braksator E, Gonzalez-Cuello A, Couch D, Hall KJ, Mundell SJ, Bailey CP, Kelly E, and Henderson G (2006) Agonist-selective mechanisms of mu-opioid receptor desensitization in human embryonic kidney 293 cells. *Mol Pharmacol* **70**:676–685.
Just S, Illing S, Trester-Zedlitz M, Lau EK, Kotowski SJ, Miess E, Mann A, Doll C, Trinidad JC, and Burlingame AL et al. (2013) Differentiation of opioid drug effects by hierarchical multi-site phosphorylation. *Mol Pharmacol* **83**:633–639.
Kelly E, Bailey CP, and Henderson G (2008) Agonist-selective mechanisms of GPCR desensitization. *Br J Pharmacol* **153** (Suppl 1):S379–S388.
Li AH and Wang HL (2001) G protein-coupled receptor kinase 2 mediates mu-opioid receptor desensitization in GABAergic neurons of the nucleus raphe magnus. *J Neurochem* **77**:435–444.
Llorente J, Lowe JD, Sanderson HS, Tsisanova E, Kelly E, Henderson G, and Bailey CP (2012) $\mu$-Opioid receptor desensitization: homologous or heterologous? *Eur J Neurosci* **36**:3636–3642.
Lohse MJ, Benovic JL, Caron MG, and Lefkowitz RJ (1990) Multiple pathways of rapid beta 2-adrenergic receptor desensitization. Delineation with specific inhibitors. *J Biol Chem* **265**:3202–3211.
Manning G, Whyte DB, Martinez R, Hunter T, and Sudarsanam S (2002) The protein kinase complement of the human genome. *Science* **298**:1912–1934.
McPherson J, Rivero G, Baptist M, Llorente J, Al-Sabah S, Krasel C, Dewey WL, Bailey CP, Rosethorne EM, and Charlton SJ et al. (2010) $\mu$-Opioid receptors: correlation of agonist efficacy for signalling with ability to activate internalization. *Mol Pharmacol* **78**:756–766.
Mundell SJ, Luo J, Benovic JL, Conley PB, and Poole AW (2006) Distinct clathrin-coated pits sort different G protein-coupled receptor cargo. *Traffic* **7**:1420–1431.
North RA and Williams JT (1985) On the potassium conductance increased by opioids in rat locus coeruleus neurones. *J Physiol* **364**:265–280.
Quillinan N, Lau EK, Virk M, von Zastrow M, and Williams JT (2011) Recovery from mu-opioid receptor desensitization after chronic treatment with morphine and methadone. *J Neurosci* **31**:4434–4443.
Raveh A, Cooper A, Guy-David L, and Reuveny E (2010) Nonenzymatic rapid control of GIRK channel function by a G protein-coupled receptor kinase. *Cell* **143**: 750–760.
Reilly SM, Chiang SH, Decker SJ, Chang L, Uhm M, Larsen MJ, Rubin JR, Mowers J, White NM, and Hochberg I et al. (2013) An inhibitor of the protein kinases TBK1 and IKK-$\varepsilon$ improves obesity-related metabolic dysfunctions in mice. *Nat Med* **19**: 313–321.
Roskoski R, Jr (2012) ERK1/2 MAP kinases: structure, function, and regulation. *Pharmacol Res* **66**:105–143.
Shenoy SK and Lefkowitz RJ (2011) $\beta$-Arrestin-mediated receptor trafficking and signal transduction. *Trends Pharmacol Sci* **32**:521–533.
Terman GW, Jin W, Cheong YP, Lowe J, Caron MG, Lefkowitz RJ, and Chavkin C (2004) G-protein receptor kinase 3 (GRK3) influences opioid analgesic tolerance but not opioid withdrawal. *Br J Pharmacol* **141**:55–64.
Thal DM, Yeow RY, Schoenau C, Huber J, and Tesmer JJ (2011) Molecular mechanism of selectivity among G protein-coupled receptor kinase 2 inhibitors. *Mol Pharmacol* **80**:294–303.
Thal DM, Homan KT, Chen J, Wu EK, Hinkle PM, Huang ZM, Chuprun JK, Song J, Gao E, and Cheung JY et al. (2012) Paroxetine is a direct inhibitor of G protein-coupled receptor kinase 2 and increases myocardial contractility. *ACS Chem Biol* **7**: 1830–1839.
Williams JT, Ingram SL, Henderson G, Chavkin C, von Zastrow M, Schulz S, Koch T, Evans CJ, and Christie MJ (2013) Regulation of $\mu$-opioid receptors: desensitization, phosphorylation, internalization, and tolerance. *Pharmacol Rev* **65**:223–254.

**Address correspondence to:** Dr. Chris P. Bailey, Department of Pharmacy and Pharmacology, University of Bath, Claverton Down, Bath BA2 7AY, UK. E-mail: c.p.bailey@bath.ac.uk